LA-4333-MS

LOS ALAMOS SCIENTIFIC LABORATORY
of the
University of California
LOS ALAMOS • NEW MEXICO

CMF-13 Research on Carbon and Graphite

Report No. 11

Summary of Progress from August 1 to October 31, 1969

UNITED STATES
ATOMIC ENERGY COMMISSION
CONTRACT W-7405-ENG. 36

This LA. . .MS report presents the summary of progress of CMF-13 research on carbon and graphite at LASL. Previous summary of progress reports in this series, all unclassified, are:

LA-3693-MS	LA-3989-MS
LA-3758-MS	LA-4057-MS
LA-3821-MS	LA-4128-MS
LA-3872-MS	LA-4171-MS
LA-3932-MS	LA-4237-MS

This report, like other special-purpose documents in the LA. . .MS series, has not been reviewed or verified for accuracy in the interest of prompt distribution.

Printed in the United States of America. Available from
Clearinghouse for Federal Scientific and Technical Information
National Bureau of Standards, U. S. Department of Commerce
Springfield, Virginia 22151
Price: Printed Copy $3.00; Microfiche $0.65

Distributed December 18, 1969

LA-4333-MS
SPECIAL DISTRIBUTION

LOS ALAMOS SCIENTIFIC LABORATORY
of the
University of California
LOS ALAMOS • NEW MEXICO

CMF-13 Research on Carbon and Graphite

Report No. 11

Summary of Progress from August 1 to October 31, 1969*

by

Morton C. Smith

*Supported in part by the Office of Advanced Research and Technology of the National Aeronautics and Space Administration.

CMF-13 RESEARCH ON CARBON AND GRAPHITE

REPORT NO. 11: SUMMARY OF PROGRESS FROM AUGUST 1 TO OCTOBER 31, 1969

by

Morton C. Smith

I. INTRODUCTION

This is the eleventh in a series of progress reports devoted to carbon and graphite research in LASL Group CMF-13, and summarizes work done during the months of August, September and October, 1969. It should be understood that in such a progress report many of the data are preliminary, incomplete, and subject to correction, and many of the opinions and conclusions are tentative and subject to change. This report is intended only to provide up-to-date background information to those who are interested in the materials and programs described in it, and should not be quoted or used as a reference publicly or in print.

Research and development on carbon and graphite were undertaken by CMF-13 primarily to increase understanding of their properties and behavior as engineering materials, to improve the raw materials and processes used in their manufacture, and to learn how to produce them with consistent, predictable, useful combinations of properties. The approach taken is microstructural, based on study and characterization of natural, commercial, and experimental carbons and graphites by such techniques as x-ray diffraction, electron and optical microscopy, and porosimetry. Physical and mechanical properties are measured as functions of formulation, treatment, and environmental variables, and correlations are sought among properties and structures. Raw materials and manufacturing techniques are investigated, improved, and varied systematically in an effort to create specific internal structures believed to be responsible for desirable combinations of properties. Prompt feedback of information among these activities then makes possible progress in all of them toward their common goal of understanding and improving manufactured carbons and graphites.

Since its beginning, this research has been sponsored by the Division of Space Nuclear Systems of the United States Atomic Energy Commission, through the Space Nuclear Propulsion Office. More recently additional general support for it has been provided by the Office of Advanced Research and Technology of the National Aeronautics and Space Administration. Many of its facilities and services have been furnished by the Division of Military Applications of AEC. The direct and indirect support and the guidance and encouragement of these agencies of the United States Government are gratefully acknowledged.

II. SANTA MARIA COKE

A. General

CMF-13 investigations of the structure, properties, behavior and potential usefulness of Santa Maria coke as a filler material for graphite manufacture have previously been summarized in the ninth and tenth reports in this series (Reports LA-4171-MS and LA-4237-MS, respectively). More recent work on this unusual raw material has been concerned principally with its grinding, molding and extrusion behavior, with some additional studies of

its structure and its response to heat treatment.

B. Internal Structure (R. D. Reiswig, E. M. Wewerka)

The unusual spheroidal units which are typical of the microstructure of Santa Maria coke were described in Report No. 9 of this series, and evidence concerning their chemical and structural nature was discussed in Report No. 10. It was concluded that the spheroids form as discrete bodies quite early in the coking process, possibly by polymerization of a specific organic component of the feed to the coker. No association of their structures with any inorganic impurity was discovered, and the possibility was also suggested that they might originate in separation of a peculiarly structured mesophase during pyrolysis of the Santa Maria refinery residue.

Mesophase separation during carbonization of a variety of coal tar pitches has been studied in detail at other laboratories, notably by Brooks and Taylor and by White et al. Typically it occurs during the last stages at which the pitch is still liquid, in a narrow temperature interval in the region of 400 to 500°C. It proceeds by formation of spherulites described as having the properties of liquid crystals, within each of which a lamellar structure exists whose geometry is such that each lamella is curved and is perpendicular both to an axis through the spherulite and to the surface of the spherulite. With time at temperature the mesophase spherulites grow and then coalesce into large ordered regions, from which lamellar coke structures are finally evolved.

Spheroids observed in Santa Maria coke appear to differ from the usual mesophase in two major respects: (1) Lamellae composing the Santa Maria spherulites appear to have grown radially from a common center rather than as curved platelets which are parallel to each other as they pass through a spherulite axis; (2) Even where their surfaces are in direct contact, the Santa Maria spherulites have not coalesced. They have apparently grown radially until they met, and then growth has ceased.

In both respects the Santa Maria spherulites resemble structures which have frequently been observed in a variety of crystalline polymers. The latter are composed of fibrils formed from chain-like molecules, folded perpendicular to the axis of the fibril. These are to be contrasted with the development resulting from nearly equiaxed, planar, aromatic molecules that separate as a mesophase from a coal tar pitch. In accordance with the polymer analogy, it can be hypothesized that the unusual spheroidal structures observed in Santa Maria coke originate in crystallization of some unidentified polymeric constituent or constituents during the early stages of coking of the Santa Maria refinery residue. This possibility is discussed in detail in a paper recently submitted to the journal Carbon for possible publication.

C. Effects of Heat Treatment on Crystalline Parameters (J. A. O'Rourke)

In preparation for the grinding experiments described below, lump Santa Maria coke was heat treated at a series of temperatures from 600 to 2800°C. For heat treatments at and below 900°C, the starting material was Santa Maria Green Coke, CMF-13 Lot No. CL-4; for higher-temperature heat treatments it was Santa Maria LV Coke, CMF-13 Lot No. CL-6. Three of the lower-temperature treatments were in vacuum and two of the higher-temperature ones were in flowing helium. In all other cases the coke was contained in an inductively heated graphite crucible which was surrounded by carbon felt, carbon black, or a combination of the two, and the atmosphere is described as "static carbonaceous". After grinding by a standard procedure discussed below, the minus 120 mesh fraction of each heat-treated sample was examined by x-ray diffraction. The measured values of crystallite thickness, L_c, and interlayer spacing, d_{002}, are listed in Table I, and L_c is plotted as a function of heat-treating temperature in Fig. 1.

As has previously been reported (in Report No. 9), heat treating the green coke at relatively low temperatures produces an initial broadening of the (002) diffraction peak and an apparent reduction in L_c. This is accompanied by a lowering of the modulated background, indicating that the line broadening results from partial reorganization of the nearly amorphous carbon originally present in the green coke.

X-ray patterns from samples heat treated at 1200,

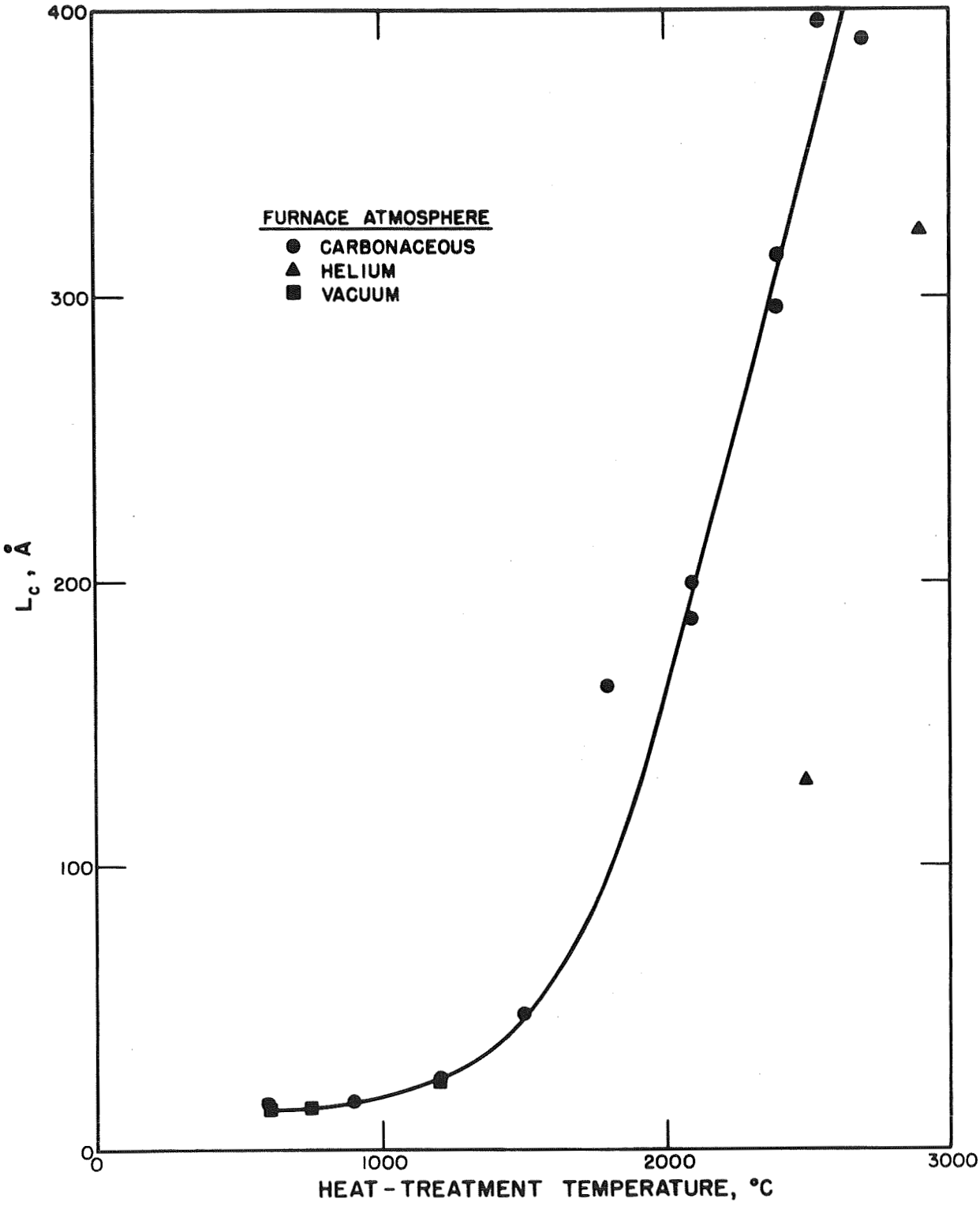

Fig. 1. Crystallite thickness, L_c, of Santa Maria coke as a function of heat-treating temperature.

TABLE I

CRYSTALLINE PARAMETERS OF HEAT-TREATED SANTA MARIA COKE

Sample Lot No.	Heat-Treating Temperature, °C	Furnace Atmosphere	L_c Å	d_{002} Å
CL-4	Green coke	---	21.7	3.45
CL-4	600	Carbonaceous	16.2	3.44
CL-4	600	Vacuum	13.8	3.44
CL-4	750	Vacuum	14.4	3.44
CL-4	900	Carbonaceous	17.7	3.44
CL-4	900	Vacuum	17.4	3.44
CL-6	1200	Carbonaceous	25.1	3.44
CL-6	1500	Carbonaceous	48.0	3.42
CL-6	1800	Carbonaceous	163	3.42
CL-6	2100	Carbonaceous	187	3.394
CL-6	2100	Carbonaceous	200	3.389
CL-6	2400	Carbonaceous	315	3.371
CL-6	2400	Carbonaceous	297	3.372
CL-6	2500	Helium	130	3.41
CL-6	2550	Carbonaceous	396	3.364
CL-6	2700	Carbonaceous	390	3.365
CL-6	2800	Helium	323	3.367

1500, and 1800°C showed definite evidence of the presence of two different -- but individually unresolvable -- crystalline distributions. These superimposed distributions are believed to have resulted in a measurement of d_{002} which was slightly low in the case of the 1500°C sample, and in too large a value of L_c for the 1800°C sample. However, there is a possibility that the latter sample was contaminated, and the 1800°C run is being repeated.

Absence of any increase in L_c between 2550 and 2700°C suggests that crystallite size is approaching some stable value near 400 Å, and this possibility will be examined. The two samples heat treated in a helium atmosphere showed crystalline growth rates somewhat lower than those of samples heated in a carbonaceous atmosphere. This too will be investigated further. The difference may result from a graphitizing influence of oxygen present in the carbonaceous atmosphere.

D. Grinding of Heat-Treated Santa Maria Coke (R. J. Imprescia)

1. Grinding Procedure: The seventeen heat-treated samples of Santa Maria lump coke listed in Table I were ground by the three-stage "S+T+I" grinding schedule, which involved successively: (1) One pass through a Williams hammer mill equipped with a screen containing 0.125-in. dia holes, at a feed rate of 90 g/min; (2) One pass through a Weber hammer mill using a screen having 0.040-in. dia holes, at a rate of 30 g/min; (3) One pass through a Trost fluid-energy mill equipped with a 1.25-in. dia discharge orifice, using 100 psi air pressure on both jets, at a rate of 15 g/min.

2. Sieve Analyses: U. S. Standard sieves were used for screen analyses of the grinding products, summarized in Table II. Heating rates for samples heated inductively in the "static carbonaceous" environment were difficult to

TABLE II

SCREEN ANALYSES OF GROUND, HEAT-TREATED, SANTA MARIA COKE[a]

Heat-Treating Temperature, °C	Furnace Atmosphere	Weight Percent in Screen Fraction (U. S. Std. Sieves)					
		+25	-25+45	-45+80	-80+170	-170+325	-325[b]
Green coke	---	0	0	0	0	0	100
600	Carbonaceous	0	0	Tr.	Tr.	Tr.	99+
600	Vacuum[c]	0	0	Tr.	Tr.	Tr.	99+
750	Vacuum[d]	0	0	Tr.	Tr.	1.0	98+
900	Carbonaceous	0	Tr.	3.5	7.5	3.0	~86
900	Vacuum[e]	0	4.0	11.0	11.5	9.5	64.0
1200	Carbonaceous	0	Tr.	6.0	12.0	8.5	73.5
1500	Carbonaceous	0	2.0	11.0	12.0	7.5	67.5
1800	Carbonaceous	0	2.0	17.0	23.0	8.5	49.5
2100	Carbonaceous	0.5	7.5	24.5	23.0	11.0	33.5
2100	Carbonaceous	0	6.0	24.0	19.0	17.5	33.5
2400	Carbonaceous	0	5.0	20.5	22.0	9.0	43.5
2400	Carbonaceous	0	6.0	26.0	18.5	12.5	37.0
2500	Helium[f]	0	4.0	16.5	10.5	16.0	53.0
2550	Carbonaceous	0	5.0	21.0	17.0	10.0	47.0
2700	Carbonaceous	0	2.5	22.5	20.0	12.5	42.5
2800	Helium	6.0	17.5	23.5	18.5	6.5	28.0
Lot G-13	As-received	0	Tr.	1.7	26.3	32.6	39.4

(a) Grinding schedule S+T+I (see text)

(b) Determined by difference

(c) 5-hr cycle

(d) 7-hr cycle

(e) 24-hr cycle

(f) Heat-treated by LASL Group CMB-6

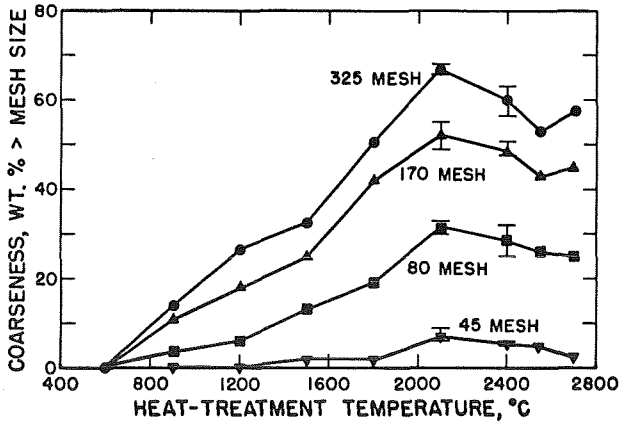

Fig. 2. Cumulative weight percent coarser than indicated screen size as a function of heat-treating temperature, ground Santa Maria coke.

control, but were fairly uniform. The screen analyses of the grinding products of samples heated in this way varied systematically and quite smoothly with heat-treating temperature, as is evident in Table II and Fig. 2. Duplicate samples heat treated at 2100 and at 2400°C gave good agreement.

Samples heat treated in vacuum at 600 and 750°C appeared to behave regularly, although the difference in their grinding behaviors was small. That heat treated in vacuum at 900°C, however, had much lower grindability than did a sample heated in the carbonaceous atmosphere to the same temperature. At least in part this may have resulted from the very low heating rate used in the vacuum

treatment, although even at the same heating rate a higher rate of removal of volatile constituents would be expected in the vacuum environment. Samples heat treated in flowing helium differed widely from those heated in the carbonaceous atmosphere both in the crystallite size produced (Fig. 1) and in their grinding behavior. This will require further investigation.

Considering only samples heat treated in the carbonaceous atmosphere, Fig. 2 demonstrates a continuous increase in the difficulty of grinding Santa Maria coke as it is calcined at progressively higher temperatures up to about 2100°C. This might be expected, since the green coke is initially quite soft and spongy and, upon heating, is transformed into a less impure but harder carbon as its volatile constituents are expelled. With heat treatment above 2100°C grindability increases, presumably because ordering of carbon atoms into a more regular graphite structure produces zones of weakness along which fracture can occur easily.

Because the slopes of the individual curves of Fig. 2 vary systematically, it is evident that -- with a given grinding procedure -- a useful degree of control over particle-size distribution is available in variation of the temperature to which the lump coke has been calcined. One object of the grinding experiments on Santa Maria coke was, if possible, to produce a particle-size distribution similar to that of CMF-13 Lot G-13, a sample of Great Lakes Grade 1008-S graphite flour, shown as the last entry in Table II. With the grinding schedule used in this investigation, this result was not achieved. However, a very important degree of control over the tendency of Santa Maria coke to break preferentially to very fine particle sizes was established. Calcination of the coke to progressively higher temperatures -- up to 2100°C -- progressively reduces the proportion of extreme fines produced by the grinding operations used here. When Santa Maria coke is to be substituted for something like the 1008-S flour, it may be desirable to calcine the coke to a temperature as high as 1900°C before grinding. Modified grinding schedules may also be desirable, to increase the proportion of material in the -170+325 mesh size interval at the expense of +80 mesh particles.

E. Micromerograph Analyses (H. D. Lewis)

A labeling error has been discovered in Fig. 6, page 9, of Report No. 10 in this series (LA-4237-MS). The points there attributed to Series VI (-80#) flour actually represented G-18 flour, and vice versa. As the accompanying text (on page 10 of that report) correctly indicated, the "size" distribution data for G-18 flour are quite well represented by a straight line on the log-probability plot, while those for all three of the Santa Maria flours show a pronounced hump in the vicinity of 10 μ.

Micromerograph particle-size data have since been collected on two other Santa Maria flours, Lots GP-14 and GP-15b, whose sieve analyses are given in Table VI. Both were prepared by grinding lump Santa Maria coke graphitized at 2700°C, using two stages of hammer-milling and one of fluid-energy milling. In both cases the -300 μ (-50 mesh) fraction was separated by screening and used for the Micromerograph analysis. Micromerograph data are plotted in Fig. 3, and show the same hump near 10 μ seen for Santa Maria flours in Fig. 6 of Report No. 10.

Sample statistics representing the data shown in Fig. 3 and based on the lognormal model are listed in Table III. Both sample distributions were characterized by large variances, leading to overestimation of $\bar{d}_3$ and $\hat{\mu}_{d_3}$ and

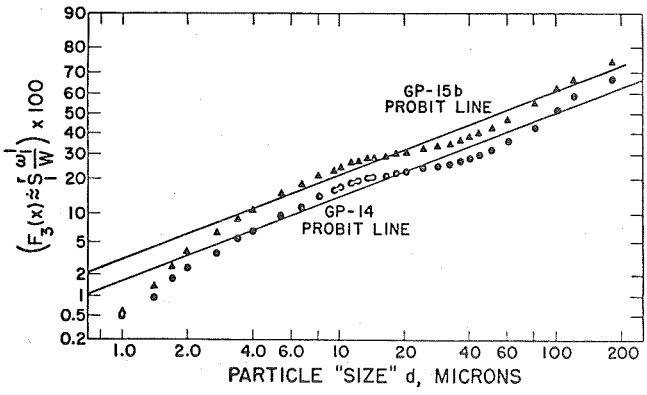

Fig. 3. Log-probability plots of Micromerograph "size" distribution data for Santa Maria graphite flour Lots GP-14 and GP-15b.

TABLE III

MICROMEROGRAPH SAMPLE STATISTICS, GRAPHITE FLOUR LOTS GP-14 AND GP-15b, LOGNORMAL MODEL

Sample	$\hat{\mu}_{x3}$	$\hat{\sigma}_x^2$	$\hat{\mu}_x$	$\hat{\mu}_{d_3}$ micron	$\hat{\mu}_d$ micron	$\hat{\sigma}_d^2$ micron^2	S_W Cm^2/gm	CV_d
GP-14	4.605	4.713	-9.536	1053.7	0.0008	0.00006	2923.	10.5
GP-15b	4.037	4.609	-9.791	567.4	0.0006	0.00003	4914.	10.0

TABLE IV

MICROMEROGRAPH SAMPLE STATISTICS, GRAPHITE FLOUR LOTS GP-14 AND GP-15b, INTERVAL MODEL

Sample	$\bar{x}_3$	s_x^2	$\bar{x}$	$\bar{d}_3$	$\bar{d}$	s_d^2	S_W	CV_d
GP-14	4.083	0.199	0.569	111.0	2.02	2.63	1527.	0.802
GP-15b	3.752	0.235	0.264	99.5	1.52	1.467	2388.	0.796

TABLE V

HELIUM DENSITIES AND SURFACE AREA STATISTICS, GRAPHITE FLOUR LOTS GP-14 AND GP-15b

Sample	Helium Density g/cm^3	BET Surface Area, M^2/g	d_s (b) Micron	Fuzziness Ratio (c) Lognormal	Fuzziness Ratio (c) Interval
GP-14	2.171 ± 0.006 (a)	9.05 ± 0.13	0.306	30.9	59.3
GP-15b	2.157 ± 0.001 (a)	11.13 ± 0.17	0.750	22.6	46.6

(a) Standard deviation of determinations.

(b) Diameter of smooth-shelled sphere having specific surface area equal to that measured by BET Method.

(c) The ratio of specific surface area measured by the BET Method to that calculated from Micromerograph sample statistics assuming smooth-shelled spheres. In this case both lognormal and interval treatments of Micromerograph data were considered.

underestimation of $\bar{d}$ and $\hat{\mu}_d$. The interval model, discussed in a later section of this report, produced the sample statistics listed in Table IV, which characterize these two materials more sensibly.

F. Helium Densities and Surface Areas (H. D. Lewis)

Helium densities and surface areas of the two Santa Maria graphite flours described above, Lots GP-14 and GP-15b, are listed in Table V. Fuzziness ratios were calculated from Micromerograph data treated both by the lognormal approximation and by the interval method. The larger numbers from use of the interval model are believed to more nearly represent the surface character of the flour particles.

G. Density-Gradient Analysis (H. D. Lewis, R. D. Reiswig)

A density-gradient column similar to that used by G. B. Engle at Gulf General Atomic has been constructed and is in operation. It was hoped that structural examination of fractions of ground Santa Maria fillers separated

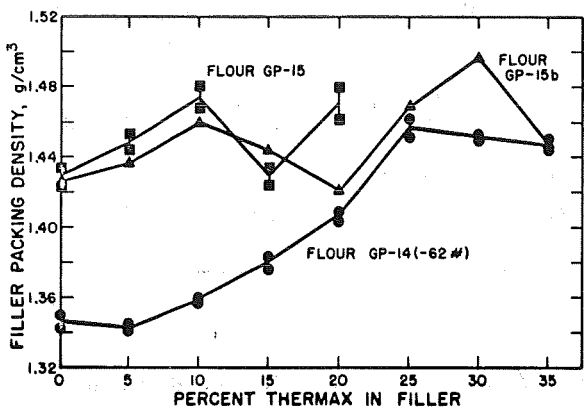

Fig. 4. The effect of Thermax carbon black additions on the packed density of molded Santa Maria graphite flours.

according to their densities might be enlightening with regard to peculiarities in their grinding behaviors. However, while a broad spectrum of particle densities has been demonstrated to exist in graphite flours GP-14 and GP-15b, the observed density differences appear to result primarily if not entirely from variations in the amount of porosity enclosed within the particles.

The technique and accompanying data analysis are being developed further and will be applied to other samples.

H. Effects of Thermax on Santa Maria Fillers

1. Packing of Molded Fillers (R. J. Imprescia)

To investigate the effect of Thermax carbon black on the packing behavior of Santa Maria graphite flours, a series of molded specimens has been made in which powdered stearic acid was used as a binder substitute and Thermax was added to the filler in 5% increments up to 35%. The principal filler materials were Santa Maria flour Lots GP-14 (-62 mesh fraction), GP-15, and GP-15b. The screen analyses of these flours are given in Table VI. Lot GP-15b was prepared from the same 2700°C-graphitized lump coke used to make Lot GP-15, and using the same grinding procedures. The two lots were very similar in screen analysis and presumably in other particle characteristics.

The stearic acid lubricant was added to each graphite flour-Thermax filler in an amount less than that which would cause die squeeze-out to occur, and the mixture was dry-blended in a twin-shell blender. Specimens were compacted by standard procedures in a steel die at 4000 psi. Duplicates of several members of the series were made and gave results which agreed well, indicating good reproducibility of materials and techniques. The behavior of Lot GP-15b was quite similar to that of Lot GP-15, as it should have been, and was quite different from that of Lot GP-14, which contained a significantly smaller proportion of fines.

Densities of the packed fillers (exclusive of the binder substitute) are plotted in Fig. 4 as functions of the weight percent of Thermax present in the filler. As would be expected, the proportion of carbon black required to achieve maximum filler density in a molded product was found to vary with the particle-size distribution of the principal filler material. At least for Lot GP-15b graphite flour, more than one density maximum may occur as the Thermax addition is increased.

TABLE VI

SCREEN ANALYSES OF SANTA MARIA GRAPHITE FLOURS

	Weight Percent in Screen Fraction (U. S. Std. Sieves)					
Lot No.	+25	-25+45	-45+80	-80+170	-170+325	-325
GP-14 (-62#)	0	Tr.	25.5	29.5	10.0	35.0
GP-15	0	Tr.	17.0	27.0	9.0	47.0
GP-15b	0	0.5	17.5	26.5	11.0	44.5

TABLE VII

MANUFACTURING DATA, EXTRUDED GRAPHITES MADE FROM SANTA MARIA GRAPHITE FLOUR PLUS THERMAX

Specimen No.	Filler Lot No.	Mix Comp., Parts by Weight			Extrusion Conditions				Green Dia in.
		Filler	Thermax[a]	Binder[b]	Pressure psi	Speed in/min	Chamber Temp, °C	Chamber Temp, °C	
ACB-1	GP-15	85	15	32.6	6750	164	50	45	0.5015
ACB-2	GP-15	85	15	33.5	4050	171	47	45	0.5015
ACG-1	GP-15b	70	30	30.9[c]	9270	160	50	65	0.505
ABY-2	GP-14 (-62#)	85	15	30	8550	156	48	45	0.5025
ACH-1	GP-14 (-62#)	75	25	29[c]	9855	167	48	54	0.5045
ACH-2	GP-14 (-62#)	75	25	30	5400	164	49	50	0.5005

(a) Thermax carbon black, Lot TP-4.

(b) Varcum 8251 furfuryl alcohol resin catalyzed with 4 wt % maleic anhydride.

(c) Appeared slightly dry.

2. Extruded Graphites Containing Thermax (J. M. Dickinson)

The extruded graphites listed in Tables VII and VIII were made using the same Santa Maria graphite flours described above, various proportions of Thermax carbon black, and Varcum 8251 furfuryl alcohol resin binder containing 4% maleic anhydride. Standard procedures were used and the graphites were extruded as 0.5-in. dia rods. Lots ACG-1 and ACH-1 were slightly deficient in binder and contained very fine edge cracks, which may have contributed to their relatively low bulk densities.

No large increase in either filler packing density or bulk density resulted from increasing the Thermax content of the filler mix to values higher than the 15% normally added. A small density increase may have occurred when the GP-14 (-62#) flour was used, but if so it was much smaller than for the molded samples discussed above.

Microscopic examination of the ACB graphites indicated that they were well mixed and well made. However, as has been common among the Santa Maria flours so far produced, the filler used was deficient in particles of intermediate size, in the range of about 20 to 30 μ. Where such particles are absent packing of coarse particles is such that relatively large spaces are left between them. These are occupied by a mixture of binder and extreme fines. Because the proportion of binder is high in these regions they shrink a great deal during curing and baking, and in the finished graphite appear as porous regions, sometimes containing colonies of relatively large voids, and frequently separated from the large filler particles by long, narrow cracks or stringers of voids. By reducing shrinkage in such regions, carbon-black particles well distributed in the binder reduce the incidence of such defects. In the ACH and ACG graphites of this series the use of additional carbon black may have reduced the porosity of the large binder volumes, but it had little apparent effect on their shrinkage away from the adjacent coarse particles or on the formation of long, narrow cracks separating them from these large particles. It appears that a gap in the size distribution in the intermediate particle size range cannot be fully corrected simply by adding more extremely fine particles to the system.

I. Warm Molding of Resin-Bonded Fillers (R. J. Imprescia)

Sound graphite specimens 3-in. dia and 1.1-in. thick have recently been produced by warm-molding a resin-bonded Santa Maria graphite flour. The filler used was CMF-13 Lot G-26, an experimental grind of a lump coke

TABLE VIII

PROPERTIES OF EXTRUDED GRAPHITES MADE FROM SANTA MARIA GRAPHITE FLOUR PLUS THERMAX

Specimen No.	Condition	Bulk Density g/cm^3	Binder Carbon Residue, %	Binder Resistivity[a] μ Ω cm	Young's Modulus[a] 10^6 psi	CTE[c], x 10^{-6}/°C With-Grain	CTE[c], x 10^{-6}/°C Across-Grain
ACB-1[b]	Cured	1.793±0.001	85.3±0.4				
	Baked	1.754±0.002	49.5±0.3				
	Graphitized	1.851±0.002	48.0±0.2	1600±11	1.83±0.01	4.76	5.03
ACB-2	Cured		84.2±0.1				
	Baked		49.0±0.2				
	Graphitized	1.847±0.001	47.7±0.2	1619±9	1.79±0.01	4.97	5.58
ACG-1[b]	Cured	1.786±0.002	87.0±0.4				
	Baked	1.729±0.003	51.3±0.3				
	Graphitized	1.838±0.002	49.9±0.3	2103±4	1.90±0.03	5.00	5.82
ABY-2	Cured	1.801±0.002	85.6±0.3				
	Baked	1.753±0.002	47.4±0.2				
	Graphitized	1.827±0.002	45.8±0.3	1665±16	1.67±0.02	4.84	5.14
ACH-1[b]	Cured	1.800±0.001	87.1±0.2				
	Baked	1.730±0.002	49.5±0.1				
	Graphitized	1.822±0.003	47.9±0.2	2065±37	1.67±0.02	5.13	5.87
ACH-2	Cured	1.793±0.002	87.1±0.2				
	Baked	1.747±0.001	49.5±0.4				
	Graphitized	1.844±0.003	47.9±0.5	1933±22	1.86±0.02		

(a) With-grain orientation.

(b) Porosity data are listed in Table XIV.

ground and graphitized at 2500°C by the Y-12 Group of Union Carbide Corporation (and identified by them as "Blend 1" of the Santa Maria flour). The binder was 23 pph of Varcum 8251 furfuryl alcohol resin catalyzed with 2% maleic anhydride. The green mix was molded in a graphite die using the following procedure: (1) Heat to 445°C at 25°C/hr under molding pressure of 4000 psi; (2) Hold at 445°C for 8 hr, maintaining this pressure; (3) Cool at 25°C/hr to 345°C, still maintaining 4000 psi; (4) Hold 1 hr at 345°C; (5) Release pressure; (6) Heat at 15°C/hr to 660°C; (7) Increase rate to 30°C/hr and heat to 900°C; (8) Hold at 900°C for 1 hr; (9) Permit to cool normally in the die to room temperature; (10) Remove from die and graphitize in flowing helium at 2800°C.

Properties of a typical specimen (No. 63F-6) produced in this way are summarized in Table IX. A degree of anisotropy is indicated which is unexpectedly high for a graphite made from a Santa Maria filler. This may result either from oriented defects or from presence of an undesirably high proportion of relatively acicular extreme fines, or from a combination of the two. Shrinkage upon graphitizing the baked specimen was 0.2% in length and 0.3% in

TABLE IX

PROPERTIES OF WARM-MOLDED,

RESIN-BONDED SPECIMEN NO. 63F-6

Condition:	Baked	Graphitized
Bulk density, g/cm^3	1.756	1.756
Packed filler density, g/cm^3	1.598	1.610
Binder residue, %	43.0	39.0
Calculated binder optimum, pph	18.6	---
Flexure strength, psi		
With-grain	---	1056
Across-grain	---	1366
Young's modulus, 10^6 psi		
With-grain	---	1.30
Across-grain	---	0.561
Internal friction, tan α x 10^3		
With-grain	---	10.2
Electrical resistivity, $\mu\Omega$cm		
With-grain	---	1533
Across-grain	---	1986

diameter.

Previous attempts to produce warm-molded, resin-bonded graphites in this and larger sizes were unsuccessful for a variety of reasons, in spite of variations in specimen size, in the filler used, and in the heating and pressure cycles. Because the inside diameter of the furnace used for these experiments is only about 8 in., die cavities greater than 3-in. dia left die-wall thicknesses less than 2.5 in., and the graphite dies exploded during the baking cycle from gas pressures developed by pyrolysis of the binder. At 3-in. specimen dia, dies exploded if specimen thickness was 1.5 in. or more, apparently from gas pressure developed within the specimen and transmitted through it to the die wall. At 3-in. dia and 1 in. thickness, specimens could be baked to 900°C under the full 4000 psi molding pressure without blowing up the die, but were found to be badly cracked radially when they were removed from the die. Radial cracking could be prevented by releasing the pressure somewhere below 500°C, but delamination cracking -- normal to the molding pressure -- occurred as the pressure was released. This again was believed to be due to gas pressure developed within the specimen. The successful cycle outlined above is believed to have eliminated these failures because it permitted slow but complete curing of the resin binder under pressure, then reduced internal gas pressure by condensing volatile gases within the specimen before the molding pressure was released, and finally permitted free escape of gases and free contraction of the specimen during baking. It is evident, however, that scaling up resin-bonded graphites of this type to thicknesses much greater than 1 in. will be difficult. The difficulties appear to be much less when pitch binders are used.

J. Extruded Resin-Bonded Graphites (J. M. Dickinson)

The same Santa Maria graphite flour described above, CMF-13 Lot G-26, has been used as the principal filler material in the series of extruded, resin-bonded graphites listed in Tables X and XI. In all cases 15 parts of Thermax carbon black were added to 85 parts of G-26 flour, and the binder was a furfuryl alcohol resin catalyzed with 4 wt % maleic anhydride. Commercial Varcum 8251 resin was used in graphite Lots ACI1, ACI3, and ACI4, and experimental resins synthesized by E. M. Wewerka, CMF-13, were used in Lots ACI2, ACI5, and ACI6. Mixing, extrusion, and heat treating of the 0.5-in. dia rods represented normal CMF-13 practice, and graphitization was to 2800°C in flowing helium.

Graphite ACI3, which contained only 23 pph of Varcum 8251, was badly deficient in binder. It cracked upon extrusion, and was discarded. Graphite ACI6 contained very small cracks, which probably influenced its physical and mechanical properties.

Among the Varcum-bonded graphites, Lot ACI4 was the best. However, the "improved" CMF-13 resins produced a density increase of about 0.03 g/cm^3, and 25 pph of resin EMW260 yielded a distinctly superior graphite. EMW260 is an undiluted acid-condensed furfuryl alcohol resin having a viscosity of 1475 cp.

K. Hot-Molded Santa Maria/Natural Graphite Mixed Fillers (R. J. Imprescia)

To explore the possibility of increasing certain of the

TABLE X

MANUFACTURING DATA, EXTRUDED RESIN-BONDED GRAPHITES

MADE FROM SANTA MARIA GRAPHITE FLOUR, LOT G-26, PLUS 15 PPH THERMAX

Specimen No.	Binder			Extrusion Conditions				Green Dia in.
	Identification	Viscosity cp	Amount pph	Pressure psi	Speed in/min	Chamber Temp, °C	Mix Temp, °C	
ACI1	Varcum 8251	250	24	6030	171	50	46	0.503
ACI2	EMW260	1475	24	11250	160	48	56	0.504
ACI3	Varcum 8251	250	23	15750	136	53	56	---
ACI4	Varcum 8251	250	25	5625	171	51	54	0.5015
ACI5	EMW260	1475	25	7875	160	49	50	0.5015
ACI6	EMW270	925	25	6750	171	48	51	0.501

TABLE XI

PROPERTIES OF EXTRUDED, RESIN-BONDED GRAPHITES

MADE FROM SANTA MARIA GRAPHITE FLOUR, LOT G-26, PLUS 15 PPH THERMAX

Specimen No.	Bulk Density g/cm^3	Binder Carbon Residue, %	Electrical Resistivity, μΩ cm		Young's Modulus[a] 10^6 psi	CTE[c], x 10^{-6}/°C		Thermal Conductivity W/Cm-°C	
			With-grain	Across-grain		With-grain	Across-grain	With-grain	Across-grain
ACI1	1.848±0.003	46.1±0.3	1703±37	1916	1.70±0.02	5.23	5.82	0.76	0.66
ACI2	1.882±0.001	48.9±0.1	1618±22	1878	1.75±0.01	4.81	5.92	0.77	0.66
ACI4	1.863±0.01	47.6±0.1	1626±22	1876	1.75±0.02	5.19	5.48	0.82	0.71
ACI5	1.894±0.004	51.1±0.1	1617±17	1881	1.78±0.02	4.66	5.26	0.78	0.67
ACI6[b]	1.891±0.002	50.6±0.1	1608±10	---	1.75±0.02	---	---	---	---

(a) With-grain orientation.

(b) Contained small cracks.

(c) Coefficient of thermal expansion, average 25-645°C.

properties of graphites made from Santa Maria fillers without seriously increasing their anisotropies, a series of hot-molded, pitch-bonded graphites has been made in which various proportions of a very fine, natural flake graphite were added to the filler. The Santa Maria filler was Lot CL-6 (described in Table II of Report No. 10 as Grinding Series VI, Schedule, S+T+U), graphitized at 2700°C. The natural graphite was Southwestern Graphite Co. Grade 1651, CMF-13 Lot No. G(Na)-21, and was 100% -325 mesh. These were solvent-blended with Barrett 30 MH coal-tar pitch, CMF-13 Lot PP-3, in the proportions indicated in Table XII, using tetrahydrofuran as the solvent. Specimens were hot-molded in graphite dies at 4000 psi, which was maintained during heating to 900°C at a constant rate over a period of 18 hr. They were graphitized in flowing helium at 2850°C.

Properties of these graphites are listed in Table XIII and plotted as functions of the natural graphite content of the filler in Fig. 5-8.

From Fig. 5, it is evident that as the fine natural graphite flakes are added they initially increase the packed density of the filler quite rapidly, by occupying spaces be-

TABLE XII

MANUFACTURING DATA, HOT-MOLDED SANTA MARIA/NATURAL GRAPHITE MIXED FILLERS

Specimen No.	Composition, Parts by Wt. Santa Maria Flour[a]	Natural Graphite Flour[b]	Coal Tar Pitch[c]	Calculated Binder Optimum pph	Binder Residue % Baked	Binder Residue % Graph.	Density, g/cm³ Bulk Baked	Density, g/cm³ Bulk Graph.	Density, g/cm³ Packed Filler Baked	Density, g/cm³ Packed Filler Graph.	Dimensional Change, Baked to Graph. % Δℓ	Dimensional Change, Baked to Graph. % Δd
61G-1	100	0	23	23.2	60.1	57.3	1.780	1.762	1.564	1.557	+0.6	-0.1
61B-1	97	3	22	23.6	60.7	57.0	1.765	1.742	1.557	1.548	+0.6	-0.0
61C-1	94	6	21	21.8	57.5	53.8	1.789	1.758	1.596	1.580	+0.8	-0.1
61D-1	91	9	20	21.5	60.1	55.7	1.793	1.766	1.601	1.589	+0.9	+0.0
61E-1	88	12	19	19.7	50.8	44.5	1.795	1.758	1.637	1.621	+0.7	+0.1
61F-1	85	15	18	21.2	60.5	54.5	1.788	1.753	1.612	1.597	+0.8	+0.1
61H-1	60	40	20	19.7	53.4	45.0	1.837	1.790	1.659	1.642	+0.9	+0.1
61I-1	30	70	20	20.6	58.3	42.9	1.854	1.776	1.661	1.636	+1.0	+0.3
59G-1	0	100	20	20.2	75.4	57.2	1.954	1.873	1.687	1.672	+1.0	-0.1

(a) CMF-13 Lot CL-6 graphitized at 2700°C.

(b) CMF-13 Lot G(Na)-21.

(c) CMF-13 Lot PP-3.

TABLE XIII

PROPERTIES OF HOT-MOLDED GRAPHITES MADE FROM SANTA MARIA/NATURAL GRAPHITE MIXED FILLERS

Specimen No.	Natural Graphite % of Filler	Density, g/cm³ Packed Filler	Density, g/cm³ Bulk	Binder Residue g/cm³	Electr. Resist. μΩcm WG[a]	Electr. Resist. μΩcm AG[a]	CTE, x10⁻⁶/°C[b] WG	CTE, x10⁻⁶/°C[b] AG	Anisotropy Ratios Electr. Resist.	Anisotropy Ratios Crystalline CTE	Anisotropy Ratios Crystalline BAF[c]	Anisotropy Ratios Crystalline M[d]
61G-1	0	1.557	1.762	0.205	1441	1568	4.87	5.78	1.09	1.19	1.063	0.34
61B-1	3	1.548	1.742	0.194	1460	1569	5.08	5.84	1.07	1.15	1.054	0.47
61C-1	6	1.580	1.758	0.178	1420	1654	5.02	6.10	1.16	1.22	1.060	0.30
61D-1	9	1.589	1.766	0.177	1412	1642	5.34	5.78	1.16	1.08	1.086	0.58
61E-1	12	1.621	1.758	0.137	1358	1755	4.63	5.90	1.29	1.27	1.106	0.67
61F-1	15	1.597	1.753	0.156	1434[e]	1764	4.49	5.44	1.23	1.21	1.109	0.52
61H-1	40	1.642	1.790	0.148	1196	1992	4.19	9.85	1.67	2.35	1.237	1.21
61I-1	70	1.636	1.776	0.140	971	3373	2.69	6.95	3.47	2.58	1.853	3.60
59G-1	100	1.672	1.873	0.201	629	3920	1.79	11.35	6.2	6.3	3.56	6.4

(a) WG = with-grain, AG = across-grain.

(b) CTE = coefficient of thermal expansion, average, 25-645°C.

(c) Bacon Anisotropy Factor, σ_{oz}/σ_{ox}.

(d) Exponent of cosine function, $I(\Phi) = I_o \cos^M \Phi$.

(e) Probably higher than true value.

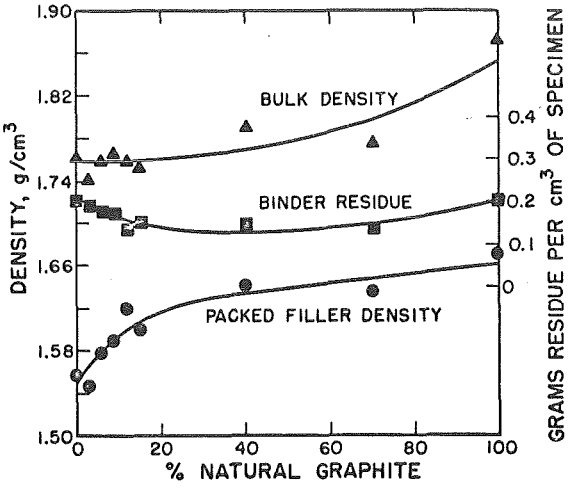

Fig. 5. Effects of natural graphite filler additions on the binder residue, packed filler density, and bulk density of molded, pitch-bonded, Santa Maria graphites.

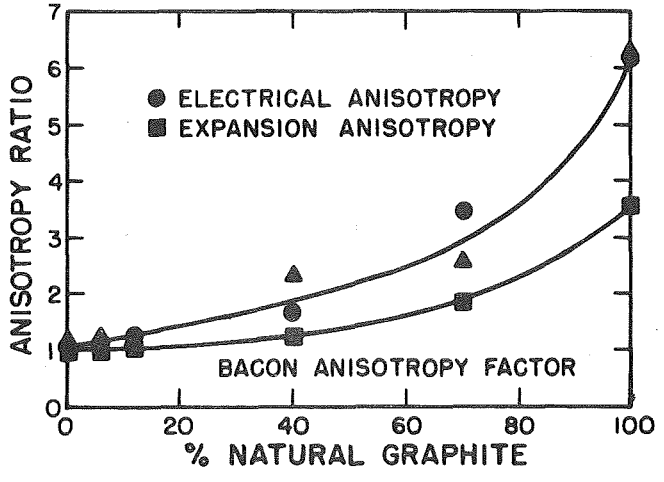

Fig. 6. Effects of natural graphite filler additions on the anisotropies of molded, pitch-bonded, Santa Maria graphites.

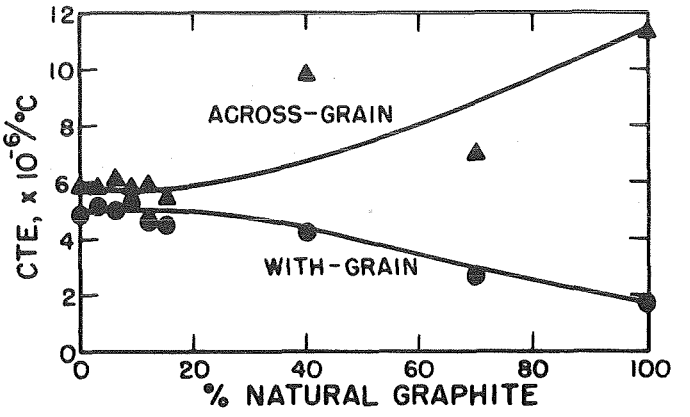

Fig. 7. Effects of natural graphite filler additions on the thermal expansion of molded, pitch-bonded, Santa Maria graphites.

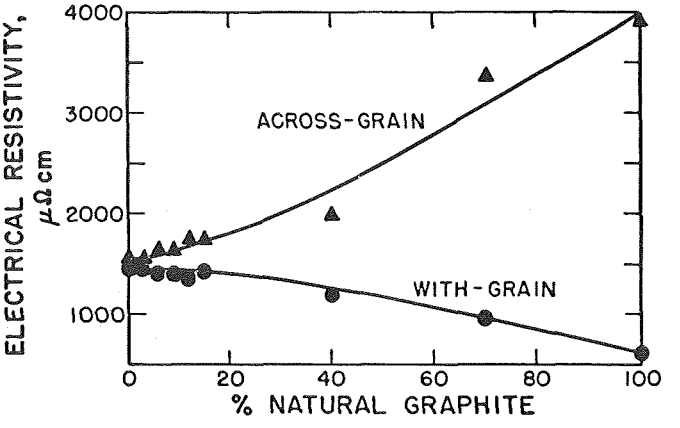

Fig. 8. Effects of natural graphite filler additions on the electrical resistivity of molded, pitch-bonded, Santa Maria graphites.

tween the larger, more nearly equiaxed particles of the Santa Maria flour. Because of filling of these spaces the binder requirement is reduced, and with it the concentration of binder residue in the finished graphite. The net effect is that bulk density remains approximately constant at about 1.76 g/cm^3 until the proportion of natural graphite becomes quite high. Above about 12% natural graphite in the filler, binder residue concentration remains approximately constant or increases, and the slow increase in packed filler density is then reflected in increasing bulk density. Part of this increase, however, is due simply to replacement of Santa Maria particles (helium density 2.16 g/cm^3) by higher-density natural graphite flakes (helium density 2.27 g/cm^3).

So long as the fine natural graphite flakes are confined mainly to interstices between the larger Santa Maria particles they have little opportunity to assume preferred orientations during molding, and anisotropy remains low--as shown in Fig. 6. However when the natural graphite be-

TABLE XIV

POROSITIES OF EXTRUDED, RESIN-BONDED GRAPHITES MADE FROM SANTA MARIA FILLERS

Specimen No.	Porosity		Pore Size Statistics							
	Total %	Accessible (> 0.082 μ) %	$\bar{x}_3$	σ^2_{x3}	g_{x3}	CV_d	Specific Surface M^2/g	$\bar{d}_3$	σ^2_{d3}	g_{d3}
ACB1-4	18.1	2.35	-0.68	0.87	1.89	0.67	15.5	1.53	35.3	1317
ABX2-6	17.48	3.69	-1.04	0.60	1.97	0.50	19.2	1.06	22.7	757
ABY2-6	19.20	3.25	-0.19	1.26	2.12	0.79	11.1	2.27	70.3	2731
ACG1-2	18.63	2.99	-1.22	0.71	2.73	0.45	23.1	1.25	40.4	1695
ACH1-2	19.29	3.71	-0.77	0.79	1.20	0.58	16.5	1.11	19.8	791
ACI-4	18.14	3.00	-0.66	0.94	1.93	0.70	15.66	1.64	39.5	1447

comes abundant enough to increase the distance between Santa Maria particles and constitute a matrix for them, then the flakes begin to orient significantly and anisotropy increases. This apparently requires of the order of 40% or more of natural graphite in the filler mixture here considered.

With-grain and across-grain thermal expansion coefficients and electrical resistivities are shown in Fig. 7 and 8 as functions of natural graphite content of the filler. Until anisotropies become quite high these properties are not much affected by the natural graphite addition. The electrical-resistivity data are of interest with regard to the statement by other investigators that this property of graphites depends principally on the binder residue and that, except as it affects morphology of the binder residue, the filler used is relatively unimportant. From Fig. 5 and Fig. 8 it is evident that the concentration of binder residue is nearly constant in a region within which electrical resistivity changes rapidly. However, the sign of this change is opposite for the two measurement orientations. When it is taken into account that in a molded graphite there are two with-grain dimensions and only one across-grain dimension, it appears that the change in bulk resistivity is actually quite small. The apparent large changes shown in Fig. 8 are primarily a result of the developing preferred orientation, and an apparent small net increase in bulk resistivity may result simply from an increase in the number of interfaces between filler particles and binder residue as the relatively coarse Santa Maria flour is replaced by the very fine natural graphite. At least for reasonably well graphitized fillers, the principal effect of the filler on electrical resistivity is apparently the result of the effects of particle size, shape, and anisotropy on the anisotropy of the graphite body produced.

None of these graphites contained gross microstructural defects. However, because of the usual deficiency of Santa Maria fillers in intermediate-size particles, most of them had, locally, relatively porous agglomerates of extreme fines and binder residue in the interstices between the larger coke particles. This was particularly evident in graphite 61G-1, to which no natural graphite was added. In mixed fillers the graphite flakes tended to occur in packets which were well aligned, with the preferred orientation of flakes composing the packets such that their c-axes were approximately parallel to the molding axis. A common minor defect was a delamination crack traversing such a packet. This defect was so common that at high magnification the packets appeared somewhat spongy and porous.

L. Porosities of Extruded Santa Maria Graphites (J. M. Dickinson)

Porosity measurements have been made on a group of extruded graphites containing Santa Maria fillers, using a mercury porosimeter to a maximum pressure of 2600 psi. Results are listed in Table XIV. The usual assumptions

were made with regard to pore shape. Statistics were calculated using the FININT (finite interval) code, and spherical pores were assumed in the calculation of specific surface.

In general these graphites have small mean pore sizes and low accessible porosities -- usually less than 4% and often less than 3%. Their pore size distributions have relatively small variances but relatively large positive skewness.

M. Young's Moduli of Santa Maria and Poco Graphites (P. E. Armstrong)

Young's modulus has been measured at room temperature on a series of specimens representing three common Poco graphites and a group of CMF-13 experimental graphites made using Santa Maria fillers. These moduli are plotted in Fig. 9 as functions of the fraction of the bulk volume of the graphite which is occupied by pores (calculated from the bulk density of each graphite). Lines of slightly different slope than that plotted for the Poco graphites would probably give a better fit to data representing the AXF and AXZ grades, but the single line shown is a reasonable correlation of the data for all three grades. Its slope is -5.155 and its intercept represents a Young's modulus at zero porosity (E_o) of 5.302×10^6 psi.

Data for graphites made from Santa Maria fillers show considerable scatter, presumably because of variations in particle-size distribution, formulation, and manufacturing procedures. However, they are reasonably well represented by the line shown, which has slope of -6.034 and the same intercept as the line representing the Poco data.

Coincidence of the intercepts of these two lines indicates that, at least with regard to elastic modulus, the graphite matrix material is essentially the same in the Santa Maria and Poco graphites. This is somewhat unexpected, since the Santa Maria graphites tested contained various resin binders and various proportions of carbon black. The greater negative slope of the line representing Santa Maria graphites indicates that, at a given porosity, the pores in the Santa Maria graphites are more effective in reducing elastic modulus than are those in a Poco graphite. This is probably explainable in terms of pore morphology. In general, at equal density, the pores in the Santa Maria graphites are finer, more numerous, more angular, and less uniformly distributed than are the pores in a Poco graphite.

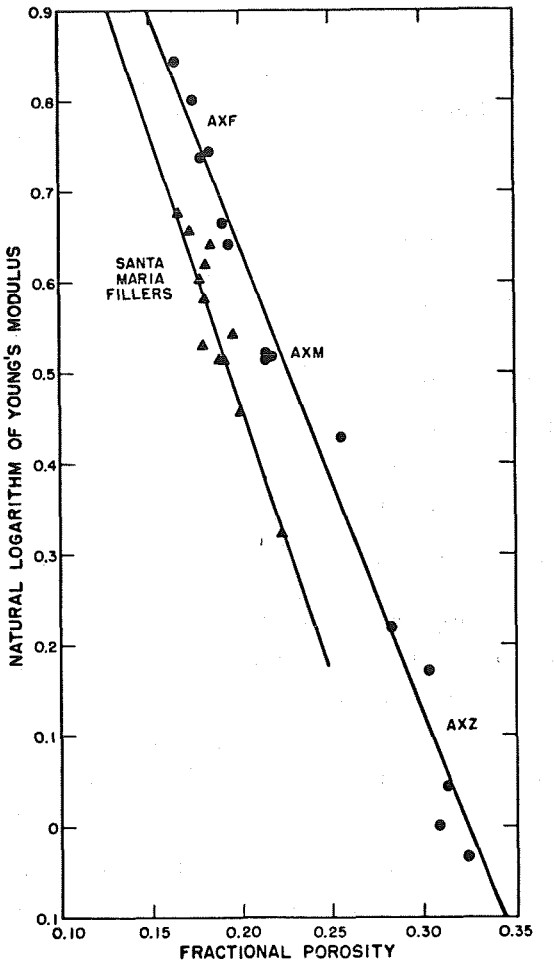

Fig. 9. Young's moduli of CMF-13 Santa Maria and of Poco graphites as functions of porosity.

N. Thermal Shock Resistance of Santa Maria Graphites (P. E. Armstrong)

Thermal shock measurements have been made in the CMF-13 focussed electron-beam heating apparatus on several of the experimental graphites mentioned elsewhere in this report. Graphite ACI1, made from a fine Santa Maria filler (Lot G-26) with a carbon-black addition and Varcum 8251 resin binder, was slightly less resistant to thermal shock than was AAQ1 graphite, a similar mater-

ial made using Great Lakes Grade 1008-S (CMF-13 Lot G-13) graphite flour as the principal filler. This would be predicted from the greater thermal expansion of the Santa Maria graphite.

III. HIGHLY ORIENTED POLYCRYSTALLINE GRAPHITES

A. General

Development of highly anisotropic manufactured graphites by CMF-13 has been discussed in Reports No. 7, 8 and 10 in this series (LA-4057-MS, LA-4128-MS and LA-4237-MS). It is hoped that polycrystalline graphites can be developed having preferred orientations such that they approach pyrolytic graphites in both ablation resistance and anisotropy of thermal conduction, and exceed pyrolytic graphite in across-grain strength and resistance to delamination.

Experimental graphites of this type have been made recently by both hot molding and extrusion.

B. Hot-Molded Anisotropic Graphites (R. J. Imprescia)

A minor but scientifically important application in which a highly oriented graphite may be useful is in targets for particle accelerators. Here energy is deposited at a very high rate by the accelerator beam, along the centerline of a long, slender, cylindrical target. Unless this energy is dissipated at an almost equal rate by radial heat flow to a cooling system outside of the target, the target material overheats very quickly. Experimental targets made from commercial graphites and tested in a LASL prototype linear accelerator have, in fact, vaporized along their centerlines. It is felt that an increase in radial thermal conductance by a factor of about two will prevent this, and that the required increase can be achieved by use of one of the CMF-13 highly oriented graphites without introducing the other danger that the target material will delaminate.

To machine targets of the present design required that a molded billet be produced not less than 2.5 in. thick normal to the preferred orientation of the layer planes of the graphite structure. The formulation selected was 85 parts CMF-13 Lot G(Na)-21 natural graphite flakes, 15 parts Thermax carbon black, and 22 pph Barrett 30 MH pitch. The mix was solvent-blended and compacted in a graphite die at 4000 psi, which was maintained during heating to 900°C over a 57 hr period and holding for 24 hr at 900°C. Graphitization was in flowing helium at 2800°C.

Two attempts to make specimens in 4-in. ID, 8-in. OD dies were unsuccessful due to die breakage during carbonization of the binder (between 400 and 550°C). A third attempt using a die 3-in. ID, 8-in. OD, was successful, apparently because of the strength increment provided by the additional die-wall thickness, and produced a sound cylinder 3-in. dia and 2.75 in. long. Density and shrinkage data and properties measured on this billet, Specimen No. 59K-4, are listed in Table XV. Of particular interest is the fact that the properties and anisotropy ratios of this material are not greatly different from those of similar but considerably thinner specimens previously produced. Graphites of this type can probably be made in thicknesses of many inches with the desired degree of preferred orientation.

Experimental targets have been cored from Specimen No. 59K-4 and will be tested in the LASL linear accelerator.

C. Extruded Anisotropic Graphites (J. M. Dickinson)

A highly oriented graphite made by extrusion will have its highest strength properties parallel to its extrusion direction, its lowest thermal conductivity normal to its surfaces, and its greatest resistance to sublimation and oxidation at these surfaces. An extruded rod or hollow cylinder of this type is expected to be useful in support structures, thermal insulators, and very high temperature tubing. Accordingly, development of highly anisotropic extruded graphites has been undertaken.

The principal filler material used in making these graphites has been a very fine (100% -325 mesh) natural flake graphite, CMF-13 Lot G(Na)-21 -- the same material used in the molded graphites previously discussed. For the ABZ series of graphites this was mixed with Thermax carbon black in the proportion of 85 parts natural

TABLE XV

PROPERTIES OF A MOLDED, PITCH-BONDED, ANISOTROPIC GRAPHITE, SPECIMEN NO. 59K-4

Bulk density, g/cm^3		Flexure Strength, psi	
Baked condition	1.881	With-grain	4949
Graphitized condition	1.832	Across-grain	1896
Packed filler density, g/cm^3		Thermal Expansion Coefficient,	
Baked condition	1.648	Ave., 25-645°C, x 10^{-6}/°C	
Graphitized condition	1.647	With-grain	2.21
Binder residue, %		Across-grain	9.23
Baked condition	64.1	Thermal Conductivity, W/cm-°C	
Graphitized condition	50.9	With-grain	1.44
Dimensional change, baked to		Across-grain	0.44
graphitized conditions, %		Electrical Resistivity, W/cm-°C	
Length	+0.3	With-grain	889
Diameter	-0.1	Across-grain	3363
Young's Modulus, 10^6 psi		Anisotropy Ratios	
With-grain	2.66	Bacon Anisotropy Factor	
Across-grain	0.71	Young's Modulus	3.75
Ultimate Tensile Strength, psi		Tensile Strength	2.26
With-grain	2655	Compressive Strength	1.30
Across-grain	1177	Flexure Strength	2.61
Compressive Strength, psi		Thermal Expansion	4.18
With-grain	5884	Thermal Conductivity	3.27
Across-grain	7647	Electrical Resistivity	3.78

graphite to 15 parts Thermax. The binders used were furfuryl alcohol resins, either commercial Varcum 8251 or an experimental CMF-13 resin, as indicated in Table XVI. Normal mixing, extrusion, and heat-treating procedures were used, and graphitization was in flowing helium to 2800°C. Properties of the finished graphites are listed in Table XVII, and porosity data on most of them in Table XVIII.

The ABZ graphites had the highly preferred orientations desired, but had low densities, high accessible porosities, and a tendency to form fine surface cracks. At least in part this was because the natural graphite filler was extremely fine, so that binder requirements for extrusion were very high. These deficiencies could probably be corrected by changing the particle size of the filler and its distribution. However, since no coarser natural graphite filler was immediately available, an attempt was made instead to modify the fine filler by adding to it a coarser, commercial graphite flour. The flour used for this purpose was Great Lakes Grade 1008-S graphite flour, CMF-13 Lot No. G-18.

Graphites ACD3 and ACD4 were made using a 3 to 1 ratio of natural graphite to commercial flour, and an 85 to 15 ratio of mixed filler to carbon black. Binder requirements were still very high, and shrinkages upon graphitization were large. Changes in properties from this modification of the mix were small.

In graphites ACD1 and ACD2, the commercial flour was the principal filler, and the fine natural graphite was used essentially as a flaky substitute for the spheroidal carbon black. (It was thought that this substitution might provide a useful, high-carbon-yield lubricant for graphites

TABLE XVI

MANUFACTURING DATA, EXTRUDED, HIGHLY ORIENTED GRAPHITES

Specimen No.	Mix Composition, Parts by Weight: Natural Graphite Flour[a]	Commercial Graphite Flour[b]	Thermax Carbon Black	Varcum 8251 Binder[c]	Extrusion Conditions: Pressure psi	Speed in./min.	Mix Temp. °C	Chamber Temp. °C	Green Rod Dia., in.
ABZ1	85	---	15	57	3600	31	42	50	---
ABZ3	85	---	15	53.2[d]	2250	7	56	45	≈0.504[e]
ACD3	63.75	21.25	15	50	2250	200	56	47	0.505
ACD4	63.75	21.25	15	45	2520	171	40	50	0.505
ACD1	15	85	---	27.3[f]	4450	---	36	50	---
ACD2	7.5	85	7.5	28	5175	164	42	45	0.510

(a) CMF-13 Lot G(Na)-21.

(b) CMF-13 Lot G-18.

(c) Including 4 wt % maleic anhydride polymerization catalyst.

(d) Experimental resin EMW (173 + 238).

(e) Surface delamination.

(f) Too dry.

which are difficult to extrude, and indeed the natural graphite did provide considerable lubrication.) Binder requirements were normal but densities were very low and accessible porosities were high. It is evident that the natural graphite flour is not acceptable as a substitute for the carbon black normally used.

Substitution of G-18 flour for part of the natural graphite was successful in several respects. Graphites ABZ1 and ABZ2, in which only natural graphite and carbon black were used, were difficult to extrude in spite of their high binder contents. Extrusion speeds were very low and the surfaces of the green rods were delaminated. Shrinkages on graphitization were large. Replacement of part of the natural graphite with G-18 flour, in Lots ACD3 and ACD4, improved extrusion behavior, reduced graphitization shrinkage, and still gave a highly anisotropic product. Other substitutions may give higher densities and better properties, and a binder having higher viscosity is probably desirable. In any case, development of an extruded, resin-bonded, highly anisotropic graphite having useful properties appears to be feasible.

Porosity data on these specimens, collected by mercury porosimetry as described above and listed in Table XVIII, shows that -- for graphites containing carbon black -- the mean pore size was smaller for the mixed fillers than for either filler used alone. ($\bar{x}_3$ is a logarithm, so that a larger negative value represents a smaller pore.) However, the smallest pore size was in Specimen ABZ3, which contained an unmixed natural graphite filler but was made with an experimental resin of considerably higher viscosity than the commercial resin. Accessible porosity was also least for this graphite, although it was not unusually low. ABZ3 also had slightly higher variance of pore sizes (σ^2_{x3}) than most of the other graphites, and a pore-size distribution which was skewed strongly toward the smaller sizes.

Microscopic examination of these graphites revealed no gross defects. The void colonies and long narrow cracks which are associated with a deficiency of intermediate-size filler particles were evident and were especially pronounced in graphite ACD1, which contained no carbon black. Graphite ACD2, to which one-half of the usual amount of Thermax was added, was improved in this regard but still contained irregular pores which were quite

TABLE XVII

PROPERTIES OF EXTRUDED, HIGHLY ORIENTED GRAPHITES

	Specimen No.					
	ABZ1	ABZ3	ACD3	ACD4	ACD1	ACD2
Bulk density, g/cm^3	1.810	1.837	1.837	1.821	1.723	1.800
Binder residue, %	40.2	41.2	42.9	40.1	40.1	43.5
Young's modulus, 10^6 psi						
With-grain	3.70	4.27	3.72	3.34	1.84	2.22
Electrical Resistivity, $\mu\Omega$cm						
With-grain	891	840	907	949	1059	1106
Across-grain	2183	---	2009	2030	1972	1953
Thermal Conductivity, W/cm-°C						
With-grain	1.56	---	1.44	1.50	1.19	1.19
Across-grain	0.60	---	0.55	0.57	0.61	0.66
Sound Velocity, 10^5 cm/sec						
With-grain	3.62	---	---	---	---	---
Across-grain	2.1[(a)]	---	---	---	---	---
CTE[(b)], x 10^{-6}/°C						
With-grain	---	---	1.30	1.44	2.05	2.34
Across-grain	---	---	4.82	5.24	4.68	5.08
Anisotropy Ratios						
Bacon Anisotropy Factor	---	---	2.58	2.11	1.646	1.616
Electrical resistivity	2.45	---	2.21	2.14	1.86	1.77
Thermal conductivity	4.06	---	2.62	2.63	1.95	1.80
Sound velocity	1.8[(a)]	---	---	---	---	---
Thermal expansion	---	---	3.71	3.64	2.28	2.17

(a) Uncertain due to extremely high signal attenuation in across-grain direction.

(b) Coefficient of thermal expansion, average 25-645°C.

TABLE XVIII

POROSITIES OF EXTRUDED, HIGHLY ORIENTED GRAPHITES

	Porosity		Pore Size Statistics							
Specimen No.	Total %	Accessible (> 0.082 μ) %	$\bar{x}_3$	σ^2_{x3}	g_{x3}	CV_d	Specific Surface M^2/g	$\bar{d}_3$	σ^2_{d3}	g_{d3}
ABZ1-6	19.91	8.14	-0.94	0.56	0.33	0.61	19.3			
ABZ3-5	18.72	4.98	-1.38	0.68	1.54	0.44	28.9	0.70	11.0	289
ACD3	18.63	6.22	-1.08	0.56	0.80	0.57	21.5	0.70	8.18	212
ACD4	19.38	7.35	-1.03	0.48	0.56	0.61	20.1	0.65	6.75	178
ACD2	20.04	8.12	-0.21	0.83	0.07	0.75	11.4	1.53	20.8	810

well interconnected.

In graphites ACD3 and ACD4, containing a high proportion of natural flake graphite, the flakes tended to occur in well-oriented packets, and delaminations within the packets were common. In several of the graphites it appeared that the graphite flakes had not been completely wet by the binder, which may result from the nature of their surfaces or may simply represent a mixing problem. In a few cases the flakes appeared to form bridges between Santa Maria filler particles and prevent penetration of binder into void spaces between them.

IV. EFFECTS OF FILLER-PARTICLE SHAPE

(J. M. Dickinson)

CMF-13 Lot AAQ1 was an extruded, resin-bonded graphite whose manufacture and properties were described in detail in a special topical report (LA-3981). The principal filler material used in it was Great Lakes Grade 1008-S graphite flour, CMF-13 Lot G-13 (identified by LASL Group CMB-6 as "M2" flour). This was combined with Thermax carbon black in the proportion 85 parts graphite flour to 15 parts Thermax, and bonded with 27 pph of Varcum 8251 furfuryl alcohol resin containing 4% maleic anhydride as a polymerization catalyst.

A subsequent shipment of Great Lakes Grade 1008-S flour, identified by CMF-13 as Lot G-18 and by CMB-6 as "M3" flour, was found to be very similar to that used in manufacturing graphite Lot AAQ1 except that its particle structure was somewhat more lamellar and its particle shapes on the average were more acicular. (Using an optical measuring system in which, by definition, the acicularity ratio of a sphere is 1.27, the acicularity ratio of Lot G-18 was 3.09, compared with 2.62 for Lot G-13.)

CMF-13 graphite Lot ACA1 has recently been produced using manufacturing procedures essentially identical with those used to make Lot AAQ1, and with the same mix formulation except that G-18 graphite flour was substituted for the less-acicular G-13 flour. Final heat-treatment temperature was 2840°C. Properties so far collected on the finished graphite are listed in Table XIX, including properties measured on individual rods. Data collected on rods 1 and 2 have been omitted in calculating the average values because, as is frequently true of the first material extruded, they are not typical of the rest of the lot.

Fifteen rods from Lot ACA1 have been sent to Southern Research Institute for use in a mechanical properties program in progress there under the direction of Dr. C. D. Pears. Data collected in that program will of course be compared with CMF-13 results and will be quoted in future reports in this series.

As was expected, Lot ACA1 is distinctly more anisotropic than was Lot AAQ1, the Bacon Anisotropy Factors of the two lots being 1.49 and 1.36 respectively. The reason for this is clear in the microstructure, in which the relatively acicular particles of the G-18 flour filler are seen to be well aligned parallel to the extrusion direction. However, with-grain electrical resistivities are nearly the same for the two lots, and with-grain Young's modulus is only slightly higher for Lot ACA1 (2.48×10^6 psi vs. 2.31×10^6 psi). Room-temperature thermal conductivity in the with-grain orientation is 1.14 W/cm-°C measured on a single rod, compared with 1.26 W/cm-°C for Lot AAQ1. This difference may be simply statistical, or may reflect the lower density of Lot ACA1 -- 1.87 g/cm^3 vs. 1.90 g/cm^3 for Lot AAQ1. Both total porosity and connected porosity were higher for Lot ACA1, made from the more acicular flour, and mean pore size was also larger. (This correlates with an observed increase in leak rates from internally pressurized, hollow, extruded shapes when the G-18 flour has been substituted for G-13.) Anisotropy ratios for Lot ACA1 were 1.84 and 1.78 for electrical resistivity and thermal conductivity respectively, compared with 1.68 and 1.68 for AAQ1 graphite. An indication of the relative resistance of the two graphites to thermal shock will be found in the next section of this report, which considers the properties of a third graphite, Lot AAP31, which is very similar to Lot ACA1.

For most purposes, use of the more acicular G-18 graphite flour instead of the G-13 flour would not be desirable.

TABLE XIX

PROPERTIES OF EXTRUDED, RESIN-BONDED GRAPHITE, LOT ACA1

X-ray Parameters:

L_c = 450 Å

d_{002} = 3.360 Å

Anisotropy Ratios:

Bacon Anisotropy Factor = 1.494

Electrical Resistivity = 1.84

Thermal Conductivity = 1.78

Sound Velocity = 1.22

Physical Properties:

Rod No.	Density g/cm^3	Carbon Residue %	Young's Modulus 10^6 psi	Electrical Resistivity $\mu\Omega$ cm	Thermal Conductivity W/cm-°C
ACA1-1	1.856	45.60	2.402	1094	
ACA1-2	1.859	46.42	2.414	1188	
ACA1-3	1.864	46.23	2.456	1167	1.14
ACA1-4	1.866	46.42	2.491	1158	
ACA1-5	1.867	46.42	2.484	1172	
ACA1-6	1.867	46.14	2.482	1178	
ACA1-7	1.868	46.46	2.474	1178	
ACA1-8	1.867	46.63	2.466	1172	
ACA1-9	1.868	46.71	2.472	1166	
ACA1-10	1.870	46.83	2.494	1176	
ACA1-11	1.871	46.60	2.492	1153	
ACA1-12	1.869	46.47	2.475	1176	
ACA1-13	1.867	46.48	2.474	1164	
ACA1-14	1.867	46.47	2.463	1182	
ACA1-15	1.870	46.60	2.494	1170	
ACA1-16	1.868	46.93	2.464	1176	
ACA1-17	1.867	46.73	2.473	1164	
ACA1-18	1.870	47.17	2.495	1164	
ACA1-19	1.873	46.92	2.526	1161	
ACA1-20	1.873	46.88	2.499	1149	
Mean	1.868±	46.6±	2.48±	1168 ± 9	
	0.002	0.3	0.02		

Porosity:

Total Porosity = 17.35% Accessible Porosity (> 0.082 μ) = 5.26%

Pore Size Statistics: $\bar{x}_3$ = -0.56 g_{x3} = -0.28 S_W = 13.5 M^2/g σ^2_{d3} = 0.43

σ^2_{x3} = 0.45 CV_d = 0.77 $\bar{d}_3$ = 0.72 g_{d3} = 2.32

TABLE XX

MANUFACTURING DATA, EXTRUDED GRAPHITES MADE WITH A VARIETY OF RESINS

Specimen No.	Mix Comp., Parts by Wt. G-18 Flour	TP-4 Thermax	Resin Binder	Binder Identification	Binder Viscosity cp	Extrusion Conditions Pressure psi	Speed in./min.	Mix Temp. °C	Chamber Temp. °C	Green Rod dia. in.
AAP31	85	15	27	Varcum 8251	≈250	6,120	164	40	52	0.504
ACE1	85	15	27	EMW-258	620	6,075	160	52	45	0.504
ACE2	85	15	27	EMW-260	1475	6,660	171	51	51	0.501

TABLE XXI

PROPERTIES OF EXTRUDED GRAPHITES MADE WITH A VARIETY OF RESINS

Specimen No.	Bulk Density g/cm^3	Binder Carbon Residue, %	Electrical Resistivity[a] $\mu\Omega$ cm	Young's Modulus[a] 10^6 psi	CTE[b], x 10^{-6}/°C With-grain	CTE[b], x 10^{-6}/°C Across-grain
AAP31	1.876	46.6	1170	2.52	2.79	4.60
ACE1	1.892	48.8	1141	2.58	2.53	4.95
ACE2	1.911	49.3	1124	2.63	2.25	4.64

(a) With-grain properties.

(b) Coefficient of thermal expansion, average, 25-645°C.

V. EFFECTS OF BINDER CHARACTERISTICS

(J. M. Dickinson, E. M. Wewerka)

A continuing program of research and development on resin binders has been discussed in several previous reports in this series. Emphasis has been on the furfuryl alcohol resins, and the conclusion has been reached that -- for this class of resins and for the type of extruded graphites made here -- the optimum binder has a viscosity in the neighborhood of 1500 cp, and a relatively narrow distribution of molecular sizes which peaks in the intermediate size range. This conclusion has been further examined by comparing the fabrication behaviors and properties of a group pf graphites made from experimental resins synthesized in CMF-13 with those of other graphites made from commercial Varcum 8251 resin. The comparison has been facilitated by using Lot G-18 graphite flour (discussed in the previous section of this report) as the principal filler material for all of these graphites, and in all cases adding to it the same proportion of Thermax carbon black (15 parts Thermax to 85 parts graphite flour).

Graphite Lot AAP31, described in Tables XX, XXI and XXII, is typical of extruded graphites made from this filler using Varcum 8251 binder. Its properties are very similar to those of Lot ACA1 described in Table XIX, indicating a high degree of reproducibility in the manufacturing and characterization techniques used.

Lots ACE1 and ACE2 were made using CMF-13 experimental resins. Both were acid-condensed furfuryl alcohol resins, but the two had widely different viscosities. Resin EMW-260 had a viscosity of 1475 cp, which is high enough to produce an extrusion pressure of almost 7000 psi and yield a green rod diameter approaching that of the die opening, 0.500 in. Resin EMW-258 had a viscosity intermediate between those of EMW-260 and the commercial resin. With increasing resin viscosity the bulk density, binder carbon residue, and Young's modulus in-

TABLE XXII

POROSITIES OF EXTRUDED GRAPHITES MADE WITH A VARIETY OF RESINS

Specimen No.	Porosity		Pore Size Statistics							
	Total %	Accessible (> 0.082 μ) %	$\bar{x}_3$	σ^2_{x3}	g_{x3}	CV_d	Specific Surface M^2/g	$\bar{d}_3$	σ^2_{d3}	g_{d3}
AAP31-4	17.08	4.55	-0.61	0.60	0.21	0.72	14.5	0.91	6.84	173
ACE1-4	16.33	3.85	-0.65	0.64	0.41	0.70	15.2	0.95	9.25	240
ACE2-4	15.35	2.45	-0.84	1.08	2.43	0.62	19.1	1.5	27.0	671

creased significantly while electrical resistivity decreased slightly and total porosity, accessible porosity, and mean pore size diminished appreciably. The density of 1.911 g/cm^3 achieved using the higher-viscosity experimental binder is exceptionally high for a graphite made from G-18 graphite flour. This and the very low accessible porosity of the graphite (2.45%) are strong arguments for the use of the high-viscosity binders. Optical and electron microscopy confirmed that Lot ACE2 was an unusually sound graphite, and had probably the best internal structure so far produced using the G-18 flour. It contained a few void stringers about 100 to 400μ long, aligned with the extrusion axis, and a few void colonies and c-face cracks. However, no major defects were discovered and the pores present were generally fine, approximately equiaxed, and well distributed. Its microstructure represented a distinct improvement over those of graphites made with lower-viscosity resin binders.

In tests in the CMF-13 focussed electron-beam apparatus, graphite AAP31 was found to be slightly inferior in thermal shock resistance to AAQ1 graphite, which was similarly made using the same formulation but with a less-acicular (Lot G-13) filler. Graphite ACE2 was slightly more resistant to thermal shock than either AAP31 or AAQ1. Apparently the high-viscosity binder used in Lot ACE2 produced an increment of thermal shock resistance sufficient to more than compensate for any reduction in this property which may have resulted from using a somewhat acicular filler.

VI. SMALL-PARTICLE STATISTICS

(H. D. Lewis)

A. Description of Non-Lognormal Particle-"Size" Data

The lognormal function in its various forms has been used by CMF-13 to approximate particle-"size" data even in instances in which it was evident that the lognormal model was not really appropriate. This was done with the realization that the sample statistics obtained were useful only for convenient comparisons of similar materials, that misleading results would be obtained in data transformations (e.g., in computing $\bar{d}$ values from weight fraction data), and that more reasonable estimates of particle-"size" distribution parameters could be derived using the finite-interval (FININT) model. In particular, it has long been recognized in CMF-13 that misuse of the lognormal model to describe truncated, large-variance sample distributions often results in a calculated $\bar{d}_3$ value greater than the diameter of the largest observed particle, and a transformed $\bar{d}$ value smaller than that of the smallest observed particle.

Lewis and Goldman were recently asked to review a paper submitted to a powder-technology journal and concerned with "weighting" of interval observations of weight fraction vs particle "size" data so that the weight-fraction mean particle diameter ($\hat{\mu}_{d_3}$ or $\bar{d}_3$) calculated from the lognormal model could not be larger than the largest observed particle. The difficulty was considered by the paper's author to result from improper weight sampling in each "size" interval, but probably in fact resulted from a misuse of the lognormal model. To help avoid such

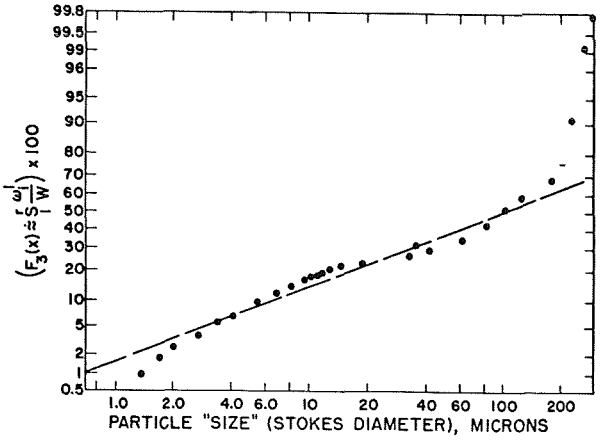

Fig. 10. Micromerograph weight-fraction data for Santa Maria graphite flour, CMF-13 Lot GP-14 (-62#).

TABLE XXIII

SAMPLE STATISTICS FOR SANTA MARIA GRAPHITE FLOUR, LOT GP-14 (-62#), COMPUTED IN THREE DIFFERENT WAYS

Lognormal Approximation	Finite Interval Calculation	Truncated Lognormal Approximation
$\hat{\mu}_{x3} = 4.604$	$\bar{x}_s = 4.083$	----
$\hat{\sigma}^2_x = 4.713$	$s^2_{x3} = 1.963$	----
$\hat{\mu}_{d3} = 1053.7$	$\bar{d}_3 = 111.0$	$\hat{\mu}_{d_3} = 73.0$
$\hat{\sigma}^2_{d_3} = 2.57 \times 10^6$	$s^2_{d_3} = 6917$	$\hat{\sigma}^2_{d_3} = 5641$
$\hat{\mu}_d = 0.0008$	$\bar{d} = 2.02$	$\hat{\mu}_d = 0.79$
$\hat{\sigma}^2_d = 0.00006$	$s^2_d = 2.63$	$\hat{\sigma}^2_d = 5.3$

difficulties and this tendency to use the lognormal model incorrectly, a truncated lognormal density function has recently been derived to describe truncated sample data which are not truly lognormal but which appear to be fitted by the lognormal function -- i.e., which gave a straight line log probability plot over a considerable size range.

For example, Fig. 10 is a log probability plot of Micromerograph weight-fraction data for the minus 62 mesh fraction of CMF-13 Lot GP-14, a finely ground Santa Maria graphite flour. The sample contained no particle larger than 300 microns dia and the smallest particle detected in the Micromerograph analysis was 0.5 micron dia. Dashed line "A" represents the probit or best lognormal fit to the data. At least qualitatively, the fit over the range 2 to 100 microns appears reasonable. However, considering the entire range of observed "sizes", the fit is obviously poor. Table XXIII compares sample statistics computed from the lognormal model, represented by line A, and from the finite interval model. As would be expected from the poor representation of data at very small and very large particle "sizes" by line A in Fig. 10, the lognormal approximation gives a value of $\hat{\mu}_{d_3}$ which is larger than the largest particle present and of $\hat{\mu}_d$ (the mean particle diameter) which is much too small. The statistics calculated from the finite interval approximation clearly represent the sample data much more accurately.

However, the lognormal model can be used to obtain better estimates of the particle-"size" distribution parameters for a sample of this type by defining a truncated density function, as follows:

For weight-fraction data,

$$f_3(x)\,(A, B) = \frac{[\, e^{3x} p(x) \,]}{\int_A^B [\, e^{3x} P(x)\, dx \,]},$$

where A and B are the lower and upper truncation points, or minimum and maximum values of ln "size" in the sample. The values of $\hat{\mu}_{d_3}$, $\hat{\mu}_d$, $\hat{\mu}'_{2d_3}$ and $\hat{\mu}'_{2d}$ are then defined as follows.

$$\hat{\mu}_{d_3} = \frac{\int_A^B e^x [\, e^{3x} p(x) \,]\, dx}{\int_A^B [\, e^{3x} p(x) \,]\, dx} = \frac{\exp[\, 4\hat{\mu}_x + 8\hat{\sigma}_x^2 \,] \int_A^B \exp\left[\frac{-[\, x - (\hat{\mu}_x + 4\hat{\sigma}_x^2) \,]^2}{2\hat{\sigma}_x^2} \right] dx}{\exp[\, 3\hat{\mu}_x + 4.5\hat{\sigma}_x^2 \,] \int_A^B \exp\left[\frac{-[\, x - (\hat{\mu}_x + 3\hat{\sigma}_x^2) \,]^2}{2\hat{\sigma}_x^2} \right] dx}$$

or, $\hat{\mu}_{d_3}$ is of the form

$$\hat{\mu}_{d_3} = \exp[\, \hat{\mu}_x + 3.5\, \hat{\sigma}_x^2 \,] \left[\frac{\int_A^B p(x; \hat{\mu}_{x4}, \hat{\sigma}_x^2)\, dx}{\int_A^B p(x; \hat{\mu}_{x3}, \hat{\sigma}_x^2)\, dx} \right].$$

$$\hat{\mu}_d = \frac{\int_A^B e^x p(x)\, dx}{\int_A^B p(x)\, dx}, \text{ or,}$$

$$\hat{\mu}_d = \exp[\, \hat{\mu}_x + .5\, \hat{\sigma}_x^2 \,] \left[\frac{\int_A^B p(x; \hat{\mu}_{x1}, \hat{\sigma}_x^2)\, dx}{\int_A^B p(x; \hat{\mu}_x, \hat{\sigma}_x^2)\, dx} \right].$$

$$\hat{\mu}'_{2d_3} = \frac{\int_A^B e^{2x} [\, e^{3x} p(x) \,]\, dx}{\int_A^B [\, e^{3x} p(x) \,]\, dx}, \text{ or}$$

$$\hat{\mu}'_{2d_3} = \exp[\, 2\hat{\mu}_x + 8\hat{\sigma}_x^2 \,] \left[\frac{\int_A^B p(x; \hat{\mu}_{x5}, \hat{\sigma}_x^2)\, dx}{\int_A^B p(x; \hat{\mu}_{x3}, \hat{\sigma}_x^2)\, dx} \right],$$

$$\hat{\mu}'_{2d} = \frac{\int_A^B e^{2x} [\, p(x) \,]\, dx}{\int_A^B p(x)\, dx}, \text{ or}$$

$$\hat{\mu}'_{2d} = \exp[\, 2\hat{\mu}_x + 2\hat{\sigma}_x^2 \,] \left[\frac{\int_A^B p(x; \hat{\mu}_{x2}, \hat{\sigma}_x^2)\, dx}{\int_A^B p(x; \hat{\mu}_x, \hat{\sigma}_x^2)\, dx} \right],$$

where $\hat{\mu}'_{2d_3}$ and μ'_{2d} are, respectively, the second moments about the origin for weight fraction and relative frequency data, required for calculation of $\hat{\sigma}^2_{d_3}$ and $\hat{\sigma}^2_{d_3}$ and $\hat{\sigma}^2_d$ for the truncated lognormal.

Using the data of Fig. 10 and the $\hat{\mu}_{x3}$, $\hat{\sigma}^2_{x3}$ values obtained from the lognormal line A, new values of mean and variance were calculated. These are listed in Table XXIII. Skewness could be calculated from the truncated model using the truncation definition of μ'_{3d_3} and μ'_{3d}, for example,

$$\hat{\mu}'_{3d_3} = \exp[\, 3\hat{\mu}_x + 13.5\, \hat{\sigma}_x^2 \,] \left[\frac{\int_A^B p(x; \hat{\mu}_{x6}, \hat{\sigma}_x^2)\, dx}{\int_A^B p(x; \hat{\mu}_{x3}, \hat{\sigma}_x^2)\, dx} \right].$$

The statistics calculated using the truncated lognormal density function are seen to represent these sample data more sensibly than does the lognormal approximation itself, and are in much better agreement with the FININT statistics. No artificial weighting or correction of observations is required, as was the case in the paper mentioned above.

The truncated density function, then, provides a useful and convenient method of estimating statistics for sample distributions of the type considered above. However, its utility is obviously limited to somewhat special conditions of truncation -- i.e., to cases in which the values of the integrals in the numerators or the denominators of the above expressions do not trend toward zero. When there is any question as to the applicability of the truncated density function, then the finite interval model should be used instead.

VII. GRAPHITE BINDERS

(E. M. Wewerka)

A. Alumina-Polymerized Furfuryl Alcohol Resins

Initial attempts to synthesize desirable furfuryl alcohol resins by distilling the monomer into a column packed with γ-alumina catalyst were not completely successful, principally because of difficulty in controlling reaction rate. To produce the desired molecular-size distribution in the resin, the polymerization must be conducted in such a way that only small amounts of unreacted furfuryl alcohol escape through the catalyst bed. However, polymerization must also be slow enough to permit efficient desorption of the low molecular weight liquid polymer from the alumina surfaces before further polymerization occurs, to prevent fouling of these surfaces by the heavier polymers. Reaction rate depends on the relative amount of effective catalyst available in the reflux column, and this depends partly on apparatus design. Several redesigns of the apparatus were required before satisfactory control of reaction rate was established. Since then several satisfactory lots of alumina-polymerized resin have been synthesized, with a wide range of viscosities.

Gel-permeation chromatography analysis of resins produced by the column-reflux method shows them to be similar in both the low molecular weight constituents present and the general shape of the molecular-size distribution curve to alumina-polymerized resins previously prepared by a continuous contact method. Unfortunately, both methods produce relatively large amounts of a material tentatively identified as difuryl either, which -- because it appears to resist further polymerization -- is believed to be detrimental to the behavior of the resin as a binder for graphite. (This conclusion is based on GPC studies of alumina-polymerized resins of varying degrees of polymerization, in all of which this component was present in a relatively high and nearly constant proportion.)

Gas-chromatography and infrared-spectroscopy analyses of a low-viscosity (350 cp) alumina-polymerized resin made by the column-reflux method have been completed. The same low molecular-weight constituents were detected as were previously identified in a commercial (Straub) resin, which is believed also to have been made by a column-reflux method. These were: furfuryl alcohol (monomer), difuryl methane, difurylether, trifuryl methane, and a still-unidentified carbonyl compound.

The properties of graphites made using alumina-polymerized resins prepared by the continuous-contact method have previously been found to be generally inferior to those of similar graphites made with acid-polymerized binder resins. Similar studies are now being conducted using alumnia-polymerized resins synthesized by the column-reflux method.

B. Scaling-Up of Resin Batch Sizes

To demonstrate the advantages of the binder resins developed by CMF-13, they must be used in the manufacture of several series of extruded and molded experimental graphites. This requires larger lots of resin than have normally been made, and scaling-up of synthesizing procedures to a batch size of about 2 kg.

A simple linear scale-up of the reaction conditions used to produce smaller resin lots was found to be unsafe for routine resin production using larger amounts of the

reactants. After some changes in apparatus and procedures, acceptable reaction conditions have now been established for production of 2 kg batches of acid-polymerized furfuryl alcohol resins. Batch-to-batch reproducibility of the resins produced is not yet as good as is desirable, and it is evident that control over certain reaction conditions must be improved. However, useful resins are now routinely produced at the 2-kg batch size, and are being used in fabrication experiments.

C. Viscosity Measurements

One important characteristic of a binder is its viscosity, and each binder resin used by CMF-13 is routinely characterized by a viscosity measurement. Until recently the instrument used to make this measurement was a MacMichael-Fisher viscosimeter, which has performed satisfactorily. However, it has recently been replaced with a Brookfield Synchro-lectric viscometer, which has several advantages. The greatest advantage of the Brookfield instrument is a design feature which permits a viscosity measurement to be made on a sample which is kept immersed in a constant-temperature bath. This minimizes the error due to temperature variations, which can be large.

Both the MacMichael-Fisher and the Brookfield instruments have been checked against a series of absolute viscosity standards and by viscosity measurements on a group of experimental resins. Both are reasonably accurate, and the two agree quite well. However, the reproducibility, accuracy, and convenience of the Brookfield viscometer are outstanding, and henceforth this instrument will be used routinely.

D. Production of Artifacts from Single Carbon Isotopes

LASL Group CMF-4 has recently begun routine production of relatively large amounts of individual carbon isotopes of high purity. These are of interest for a wide variety of applications, including possible use to produce carbon artifacts containing a single isotope -- to be used, for example, as beam stops in a particle accelerator.

The individual carbon isotopes are separated by CMF-4 as carbon monoxide. Presumably this can be hydrogenated to produce methane, which can be pyrolyzed to produce pyrolytic carbon or pyrolytic graphite. Isotopically pure pyrocarbon or pyrographite will be directly useful in some cases. However, where shapes are such that radii are small, when orientation of the graphite structure must be controlled, when delamination must be avoided, or a high degree of anisotropy is undesirable, then a polycrystalline graphite would be preferred. This would require separate development of a filler, a binder, and a fabrication procedure.

Given a supply of massive pyrocarbon or pyrographite, CMF-13 has already developed the techniques for producing a highly oriented polycrystalline graphite from it. If such a graphite were required, as it probably would be for a beam stop, two principal further developments would be necessary: development of a facility for hydrogenating isotopically pure CO to CH_4 and of pyrolyzing the CH_4 to massive pyrocarbon or pyrographite; and development of procedures for synthesizing a suitable binder from CO. If less anisotropic graphites were required, it would also be necessary to develop procedures to synthesize a precursor which, upon pyrolysis, would yield a less well-ordered carbon filler than either pyrocarbon or pyrographite.

Because of these interests and possibilities, a preliminary literature search has been made to identify some possible synthetic routes to appropriate binder materials -- some of which might also be useful as precursors for production of carbon fillers.

The binder materials which have been used by CMF-13 have been chiefly coal-tar pitches and furfuryl alcohol resins. An additional, but less familiar, possibility is a phenol-formaldehyde resin. Since a high degree of flexibility is desirable at this point with regard to the type of graphite made and the fabrication procedures used to make it, all three of these binder types have been considered. If and when a specific product requirement is established, a fabrication method will be outlined and the most practical route to synthesis of an appropriate binder will be established by a more thorough literature search, by consultation with other chemists, and by the necessary laboratory

investigations. Preliminary schemes have been worked out for synthesis of furfuryl alcohol resins, phenolic resins, and synthetic pitches, with several alternative routes to each. A considerable development period would be required to identify the best and shortest routes, to establish reagent requirements and reaction conditions, and to demonstrate procedures using ordinary materials. However, it is already evident that development and production of isotopically pure graphites is feasible, and the development does not appear to involve any really formidable problems.

VIII. PHYSICAL PROPERTIES

(P. E. Armstrong)

A. Low-Temperature Resistivity of Boron-Doped Graphites

Electrical resistivity has been measured as a function of temperature over the range 4.2°K to 300°K on a series of 0.25-in. dia specimens machined from the boron-doped, extruded graphite rods previously examined at higher temperatures by P. Wagner. For the undoped reference graphite in the series, resistivity was found to increase by 85% as temperature was reduced from 300 to 4.2°K. For all of the boron-doped graphites, the resistivity change over this temperature range was less than 10%. Several minima appeared in the resistivity vs temperature curve for each boron-doped graphite. Because the measurements were made with the specimens in direct contact with nitrogen and helium vapor and with no prior evacuation, it is possible that the results were influenced by the presence of absorbed or adsorbed water. The experiments will therefore be repeated. If indeed the resistivity changes observed are associated only with boron content of the graphite, they may indicate interesting changes with temperature in the nature of the electrical conduction.

B. High-Frequency Sound-Velocity Measurements

The high-frequency pulse-transmission method of measuring sound velocity can be applied satisfactorily to specimens as small as 0.150-in. thick and less than 0.5-in. dia. Velocity measurements can therefore be made both with-grain and across-grain on relatively small graphite samples, such as the 0.5-in. dia extruded rods commonly produced in CMF-13. It appears that the anisotropy ratios from velocity measurements should correlate with anisotropies of other properties. This possibility is being investigated by high-frequency sound-velocity measurements on a series of small specimens machined from samples of various CMF-13 graphites on which other physical and mechanical measurements are also being made.

IX. DEFORMATION MECHANISMS

A. Theoretical (J. Weertman)

A theory has been developed to account for the high-temperature creep of any graphite which contains small cracks (as all manufactured graphites do). This theory is based on a dislocation-climb mechanism.

It is assumed that when cracks in graphite are subjected to a tensile force, edge dislocations are nucleated at their tips. These dislocations move away from the crack tips with a climb motion. As they climb, lattice vacancies are created which diffuse away from the dislocations to the crack surfaces, where they are destroyed in creating new surface. The ultimate rate-controlling process in this creep model thus is self-diffusion. The model therefore can explain the observation discussed below that the activation energy for creep is approximately equal to that expected for self-diffusion.

For the initial stage of creep, the theory gives the following equation:

$$\epsilon - \epsilon_o \cong (2\pi^2 w N \sigma_A/3)\,(VD/\bar{\mu} k T)^{\frac{1}{3}} t^{\frac{1}{3}} \qquad (1)$$

where: ϵ = total strain

ϵ_o = initial, instantaneous strain

w = half-width of infinitely long cracks

N = number of infinitely long cracks per unit area. (For cracks of finite length 2w, the expression wN in the equation is replaced with w^2N, where N is now the number of

cracks per unit volume.)

σ_A = applied tensile force per unit area

V = the factor which, when multiplied by the interatomic distance, is equal to the atomic volume of a carbon atom

D = self-diffusion coefficient

$\bar{\mu}$ = average shear modulus

k = Boltzmann's constant

T = absolute temperature

t = time

The number, N, of active cracks can be a function of stress.

Equation (1) is valid to strains of the order of $\varepsilon \approx 3$ to $10\,\varepsilon_o$, where

$$\varepsilon_o = N\,(\sigma_A/\bar{\mu})\,w^2\,(\pi^2/2). \qquad (2)$$

At greater strains the creep strain becomes proportional to t rather than $t^{\frac{1}{2}}$.

The creep model which leads to Equation (1) also predicts that, if the tensile load is removed, creep recovery will occur. In the initial stage of recovery, the creep strain recovered is again proportional to $t^{\frac{1}{2}}$, where t is time after load removal.

B. Experimental (W. V. Green, E. G. Zukas)

The validity of Equation (1) is being evaluated by comparing its predictions to experimental behavior in the following ways:

1. The theory relates creep strain to time, stress, and temperature. The creep strain predicted by it at a given time can be compared with that measured experimentally in a test made at known temperature and load per unit area. Unfortunately, the single-crystal elastic constants required to calculate $\bar{\mu}$ are not known at creep temperatures. From the known lattice parameters at temperature and the Lennard-Jones potential with respect to displacement, it was estimated that at 2500°C the value of $\bar{\mu}$ would be 0.27 of its room-temperature value. Using this, Equation (1) predicts that, after 2 to 3 hr at 2500°C under tensile stress of 4500 psi, a graphite initially containing small cracks will have extended about 5%. This elongation is indeed typical of these creep conditions.

2. Equation (1) predicts that up to strains of the order of $10\,\varepsilon_o$, total strain will be a linear function of $t^{\frac{1}{2}}$, and that recovery strain will have this same time-dependence. Experimental creep and recovery data plotted for a variety of temperatures and creep stresses is indeed approximately linear with $t^{\frac{1}{2}}$, and is less well represented by $t^{1/3}$ or $t^{2/3}$.

3. The t=0 intercept of a plot of ε vs $t^{\frac{1}{2}}$ is ε_o. The ε_o term includes not only a purely elastic (Young's modulus) term, but also a crack-opening term. The stress-dependence of creep strain is contained in the term $2\pi^2 wN\sigma_A/3$. If the crack-opening contribution can be related to wN and both of these related to σ, then this will indicate that the dependence of creep strain on stress is correctly represented by Equation (1).

By determining a stress vs. strain diagram at low stresses and at a temperature just low enough so that no significant time-dependent strain occurs during loading, it is possible to measure ε_o directly. Results from such measurements will be compared with values of ε_o determined graphically from creep data.

Microstructural studies previously reported have already established that w is nearly constant, as is assumed in Equation (1). Absolute creep rates have been calculated for values of w computed as the critical size of a Griffith crack, and the computed rates are comparable to experimental ones.

The apparent activation energy for creep, Q_c, has been measured experimentally many times, usually by the "Δ T" method in which, during the creep test, the temperature is changed suddenly while stress is held constant. Barrett, Ardell and Sherby (Trans. Met. Soc. AIME 230, 200, 1964) have proposed a correction to Q_c determined in this way, required because the test is made at fixed stress instead of at a fixed ratio of stress to elastic modulus. Using the estimate of elastic modulus mentioned above, this correction is computed to be 54 kcal/mole, which is to be applied to an average experimental value of about 250 kcal/mole for creep of graphite in the neighbor-

hood of 2500°C. The resulting corrected value of Q_c agrees very well with an average value of about 190 kcal/mole previously determined as the apparent activation for creep recovery -- to which no stress/modulus correction need be applied. It agrees equally well with the activation energy of 190 kcal/mole reported by Thrower (Phil. Mag. 18, 697, 1968) for annealing out of point defects produced in graphite by irradiation. Since annealing out of point defects is presumably controlled by self-diffusion, the agreement among these three activation energies is evidence in support of the deformation model on which Equation (1) is based.

X. PUBLICATIONS RELATING TO CARBONS AND GRAPHITES

Smith, M. C., "CMF-13 Research on Carbon and Graphite, Report No. 10, Summary of Progress from May 1 to July 31, 1969", LASL Report No. LA-4237-MS, September, 1969.

Armstrong, P. E. and Eash, D. T., "Simultaneous Measurement of Young's Modulus and Shear Modulus at Low Temperatures", Advances in Cryogenic Engineering, Vol. 14, pp. 64-70, June, 1969.

Wagner, P., O'Rourke, J. A., Dickinson, J. M., and Dauelsberg, L. B., "Thermal Conductivity of a Graphite Rod", Abstract in: Thermal Conductivity, 1968, 8th Conference, Purdue Univ. Proceedings, p. 571, Plenum, 1969.

Bard, R. J., Baxman, H. R., Bertino, J. P., Hayter, S. W., O'Rourke, J. A. and McCreary, W. J., "Development of Particles Coated with Pyrolytic Carbon. VIII. Improved Core-Coat Combinations", CONFIDENTIAL LASL Report No. LA-4308, Dec. 3, 1969.